Accepted Manuscript

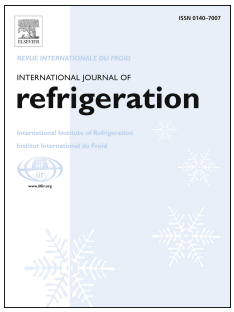

Pre-industrial development and experimental characterization of new air-cooled and water-cooled ammonia/lithium nitrate absorption chillers

Miguel Zamora, Mahmoud Bourouis, Alberto Coronas, Manel Vallès

PII: S0140-7007(14)00154-6

DOI: 10.1016/j.ijrefrig.2014.06.005

Reference: JIJR 2810

To appear in: *International Journal of Refrigeration*

Received Date: 14 February 2014

Revised Date: 3 June 2014

Accepted Date: 6 June 2014

Please cite this article as: Zamora, M., Bourouis, M., Coronas, A., Vallès, M., Pre-industrial development and experimental characterization of new air-cooled and water-cooled ammonia/lithium nitrate absorption chillers, *International Journal of Refrigeration* (2014), doi: 10.1016/j.ijrefrig.2014.06.005.

Pre-industrial development and experimental characterization of new air-cooled and water-cooled ammonia/lithium nitrate absorption chillers

Miguel Zamora[a], Mahmoud Bourouis[b*], Alberto Coronas[b], Manel Vallès[b]

[a] *CIAT Air Thermodynamics R&D Department. Pol. Llanos de Jarata s/n 14550 Montilla, Cordoba, Spain*

[b] *Department of Mechanical Engineering, Universitat Rovira i Virgili, Av. Països Catalans No. 26, 43007 Tarragona, Spain*

* *Corresponding Author (Email: mahmoud.bourouis@urv.cat; Phone: +34 977 55 86 13; Fax: +34 977 55 96 91)*

Abstract

Two pre-industrial prototypes of a new ammonia/lithium nitrate absorption chiller, a water-cooled one and an air-cooled one, have been built and experimentally characterized. The single-effect configuration of the absorption refrigeration cycle was selected for both prototypes in which brazed plate heat exchangers were used in all thermal components. These prototypes, designed for air conditioning applications, were tested under various operating conditions to assess their performance. The water-cooled prototype yields 12.9 kW of cooling capacity and an electrical COP_{elec} of 19.3, when operating at a 15 ºC chilled water temperature, 90 ºC hot water temperature and a 35 ºC cooling water temperature. In the case of the air-cooled prototype, at a 15 ºC chilled water temperature, 90 °C hot water temperature and a 35 °C ambient air temperature, the cooling capacity is 9.3 kW and the electrical COP_{elec} is 6.5.

Keywords: Absorption chiller, ammonia, lithium nitrate, plate heat exchanger

Highlights

- Two pre-industrial prototypes of a new ammonia/lithium nitrate absorption chiller were developed and experimentally characterized.
- Brazed plate heat exchangers were used in all thermal components.
- A water-cooled prototype and an air-cooled one were tested under various operating conditions.

Nomenclature

BPHE:	Brazed Plate Heat Exchanger
COP:	Coefficient of Performance
EEV:	Electronic Expansion Valve
F:	Fan rotation speed (r.p.m)
LMTD:	Logarithmic Mean Temperature Difference (ºC)
P:	Pressure (bar)
Pw:	Electrical power input (kW)
Q:	Thermal power (kW)
RHX:	Refrigerant Heat Exchanger
SHX:	Solution Heat Exchanger
T:	Temperature (ºC)

Subscripts

AC:	Refers to absorber/condenser
AIR:	Refers to ambient air
E:	Refers to evaporator/evaporation
elec:	Electrical
G:	Refers to generator/generation
Hyd:	Hydraulic power of the circulation water pump due to pressure drop in a heat exchanger
pump:	Refers to solution pump
ther:	Thermal
w:	Refers to water side
1:	Inlet to the chiller (*)

2: Outlet from the chiller (**)

(*) When not indicated, T_E denotes chilled water outlet temperature

(**) When not indicated, T_G, T_{AC}, T_{AIR} denote temperatures at the chiller inlet

Greek letters:

$\dot{v}$: Volumetric flow ($m^3 \cdot h^{-1}$)

ε: Heat Exchanger Efficiency

ΔP: Pressure drop (bar)

η: Pump efficiency

Introduction

During the first decade of this century several low capacity absorption chillers have appeared on the European scene focused especially on solar thermal cooling applications for the residential sector. The majority were single-effect units using the water/lithium bromide working pair as the ROTARTICA, PHONIX or WEGRACAL products. Other consolidated manufacturers of large scale absorption chillers such as YAZAKI, THERMAX and BROAD have also extended their product range to cooling capacities lower than 30 kW. These single-effect absorption chillers can be activated with hot water at low temperatures (i.e. 80 to 95 ºC), produced by flat solar collectors, and can achieve a thermal coefficient of operation (COP_{ther}) of 0.7.

Another innovative cooling machine that has additionally experimented good commercial diffusion is the CLIMATEWELL adsorption machine that operates with water/lithium chloride as a working pair.

Moreover, the traditional working pair ammonia/water has also been used in solar cooling applications with single-effect cycle configurations such as those in the chillers manufactured by PINK and AGO. On the other hand, gas-fired ammonia/water absorption chillers have always been present in cooling applications, with manufacturers like ROBUR keeping a steady presence in the sector over the years. Nowadays, the GAX (Generator-Absorber-Exchanger) thermodynamic cycle is employed in these gas-fired absorption chillers.

A review of all of these new machine concepts can be found in Marcos (2008), Jakob and Kohlenbach (2009) and Deng et al. (2011).

The most important drawback of water/lithium bromide technology is the risk of crystallization at high absorber temperatures. Because of this commercial chillers that use this working pair are commonly water-cooled, hence requiring cooling towers. Air-cooled machines with water/lithium bromide are still scarce; the ROTARTICA machine equipped with a dry cooler was an exception because of its particular rotary operation. The need for a cooling tower introduces a certain rejection in the residential HVAC market because of the higher maintenance costs which are necessary to avoid risk of Legionella. Different research efforts have been conducted in this field such as those reported by Kim and Machielsen (2002), Kim and Infante Ferreira (2009) and Gonzalez-Gil et al. (2011).

Ammonia/water GAX chillers can be air-cooled but they require higher activation temperatures, which makes the use of the cheaper flat solar collectors impossible in solar cooling applications.

In this context, the HVAC manufacturer CIAT and the CREVER research group from the Rovira i Virgili University, launched a research and development project for a new

absorption chiller of 10 kW of nominal cooling capacity using the ammonia/lithium nitrate mixture as a working pair. Between 2006 and 2011 two laboratory prototypes and two pre-industrial prototypes were manufactured and tested using BPHE in all the thermal components (Zamora et al. 2011).

In comparison with the water/lithium bromide absorption chillers that operate under vacuum, the assembly process of ammonia absorption chillers is more similar to the technique employed in the vapour compression chillers which operate under pressure. Furthermore, an ammonia/lithium nitrate absorption chiller does not require a rectifier while an ammonia/water chiller does. This reduces the machine weight and cost. However, in order to be competitive with vapour compression chillers, there are still some drawbacks of ammonia absorption chillers that must be overcome. Firstly, though the running cost of the absorption refrigeration system is much lower than that of the vapour compression system, its initial capital cost is still much higher. Secondly, the refrigerant charge must be reduced to its minimum, due to the ammonia toxicity.

Nowadays, Brazed Plate Heat Exchangers (BPHEs) are the most common heat transfer geometry used in compression chillers due to their compactness and lower system refrigerant charge and cost.

This paper presents the current work carried out, showing the most significant results achieved during the development of the aforementioned new absorption chiller.

Ammonia / lithium nitrate absorption refrigeration systems

Ammonia/lithium nitrate mixture has been reported as a working pair for absorption refrigeration systems since the first half of the twentieth century. The English patent 358.844 claimed the thermodynamic design of an absorption chiller using ammonia as

refrigerant and a solution of ammonia with an anhydrous non-volatile salt, such as lithium nitrate as absorbent (Electrolux LTD, 1930). Its interest for solar cooling applications took off after the research performed by Infante Ferreira (1984) who published a new set of equations for the equilibrium properties (P-T-x and h-T-x curves). This working fluid does not present risk of crystallization when operating at high temperatures in the absorber, thus makes it suitable for dissipating the heat released in the condenser and absorber using air and without cooling tower. This is an advantage compared with the conventional water/lithium bromide technology.

Libotean et al. (2007 and 2008) published the equilibrium properties and transport properties, namely the density, heat capacity and dynamic viscosity of the ammonia/lithium nitrate solution. With these thermophysical properties the thermodynamic cycle operating with this working fluid can be modelled and the different components of the chiller can be sized for a given cooling capacity.

By means of numerical simulation, Sun (1998) compared the thermal coefficient of performance (COP_{ther}) with other ammonia based mixtures, namely ammonia/sodium thyocianate and ammonia/water mixtures. Ammonia/sodium thyocianate offered a slightly higher COP_{ther}, but required a higher minimum activation temperature. For high heat rejection temperatures, ammonia/water requires a generation temperature of at least 10 ºC higher than the two other ammonia/salt mixtures. For this reason, nowadays commercially available air-cooled ammonia/water absorption chillers are gas-fired using the GAX cycle configuration, while the aforementioned single-effect absorption chillers are water-cooled.

In the last few years, the use of plate heat exchangers in ammonia absorption refrigeration systems has been reported in the open literature. Cerezo (2006) studied the absorption process of ammonia/water in BPHEs, while Táboas (2007) conducted

research on the generation process of ammonia/water in BPHEs. Oronel (2010) using the same benches studied the absorption and generation processes of the ammonia/lithium nitrate pair in BPHEs.

Venegas et al. (2005), Ventas et al. (2010) and Zacarias et al. (2011) have carried out research works on the adiabatic absorption of the ammonia/lithium nitrate mixture employing a BPHE for subcooling the poor solution in ammonia before spraying it inside an adiabatic absorber. Amaris et al. (2011) have experimentally investigated the bubble absorption process in a tubular geometry. This research topic is very relevant as performing the absorption process inside a tubular geometry would allow the use of finned tube heat exchangers for the absorber of absorption chillers.

Heard et al. (1994) modified an experimental 10.5 kW ammonia/water absorption cooler to use ammonia/lithium nitrate as a working pair. This prototype charged with $NH_3/LiNO_3$ was tested at generator temperatures ranging from 90 ºC to 140 º C, evaporator temperatures down to -20 ºC and condensation temperatures between 10 ºC and 35 ºC. The cooling capacity was reduced to approximately half the design value and the maximum COP of 0.4 was obtained when operating with ammonia/lithium nitrate as a working pair.

In 2009, the CIAT group presented a patent of the first ammonia/lithium nitrate absorption chiller built using BPHEs in all its thermal components, including the absorber and the generator (Bourouis et al. 2009). A special distribution device for mixing the ammonia vapour and the poor solution at the absorber entrance port was patented.

Llamas et al. (2011) have performed experiments on an air-cooled 5 kW ammonia/lithium nitrate absorption cooling prototype, which incorporates a vertical

tubular falling film absorber. The first results showed thermal performance below the expected values, with COP values of 0.35-0.40 and cooling loads in the range of 3 to 5 kW.

Description of the constructed absorption chiller prototypes

The nominal design parameters considered for the prototype developed in this work were as follows: cooling capacity (Q_E) of 10 kW at chilled water outlet temperature (T_{E2}) of 15 °C, hot water inlet temperature (T_{G1}) of 90 °C and cooling water inlet temperature (T_{AC1}) of 37.5 º C.

The cycle configuration of the developed absorption prototypes is shown in Figure 1 and briefly described in this section. The ammonia vapour coming from the generator enters in the condenser (1) which consists of a one-pass BPHE with a heat transfer area of 0.96 m^2 and through it circulates cooling water for removing the heat of condensation. The liquid refrigerant is stored in the receiver (2). From this receiver, the refrigerant liquid enters in the one-pass BPHE refrigerant heat exchanger (RHX) (3), with a heat transfer area of 0.12 m^2, where it is sub-cooled before its expansion by the electronic expansion valve (EEV) (4). The low pressure vapour-liquid mixture coming from the EEV (4) enters in the one-pass BPHE evaporator (5) with a heat transfer area of 1.08 m^2. The evaporation heat produces the chilling effect, after which the ammonia vapour returns to the RHX (3) where it is preheated.

The preheated vapour refrigerant is mixed with the poor solution in the inlet port of the absorber (7) due to a distribution system (6) specifically designed by the authors for the developed prototypes. The absorber (7) is a one-pass BPHE with a heat transfer area of 2.04 m^2, in which the bubble absorption of the ammonia in the poor solution takes place

in the upwards channels and the absorption heat is removed by the cooling water circulating in counter-current configuration through the downward channels.

The rich solution coming out of the absorber (7) is accumulated in the tank (8), from where it is pumped by the solution pump (9) to the solution heat exchanger (SHX) (10) for heat recovery between the hotter poor solution and the colder rich solution. The SHX (10), for which a high efficiency ($\varepsilon > 0{,}85$) is recommended, consists of a two-pass BPHE heat exchanger with a heat transfer area of 2.1 m^2. From the SHX (10) the rich solution enters in the one-pass BPHE generator (11), with a heat transfer area of 1.44 m^2, in which the desorption process is started, making use of the heat supplied by hot water. The ammonia vapour and the solution leaving the generator are conducted to the separation tank (12) where the two phases are separated.

The poor solution coming from the bottom part of the separation tank (12) circulates through the SHX (10) to the solution expansion device (13). This is a self-regulated expansion device consisting of a calibrated orifice and driven by a membrane. From the expansion device (13), the low pressure poor solution returns to the inlet port of the absorber.

The pure ammonia vapour leaves the separation tank (12) from its upper side, going to the condenser (1), and closing the single-effect absorption thermodynamic cycle.

In the air-cooled prototype, the absorption and condensation heat removed by cooling water is dissipated in a finned tube heat exchanger (14) which is integrated into the unit.

The water-cooled prototype is not equipped with a heat rejection system. For instance, an external cooling tower can be used.

Data reduction

The experimental campaign was carried out on a test bench at the CREVER Laboratory of Rovira i Virgili University. The performance of the air-cooled prototype was characterized in a climatic chamber (Figure 2). The test matrix is summarized in Table 1.

Cooling capacity, generation power and heat rejection power were calculated from energy balances using the temperatures measured by Pt-100 sensors of ±0.1 K precision located at the inlet and outlet of the water circuits and the water flows measured with flow meters of ±0.5 % precision. The uncertainty of determining the cooling capacity and generation power is 0.5 kW. For the air-cooled prototype neither the cooling water flow nor the air-flow were measured, so that heat rejection power was estimated by performing the overall energy balance. Air temperature was also measured with six thermocouples located at the coil inlet and two other thermocouples located at the fan outlet.

As there is no specific standard for this type of absorption chillers, the following standards were employed: EN 12309-2:2000 entitled "Gas-fired absorption and adsorption air-conditioning and/or heat pump appliances with a net heat input not exceeding 70 kw. Part 2: Rational use of energy" and prEN 14511-3:2011 entitled "Air conditioners, liquid chilling packages and heat pumps with electrically driven compressors for space heating and cooling. Part 3: Test methods".

The cooling capacity and the absorbed electrical power were corrected taking into consideration the consumption of the chilled water circulation pump, as indicated in prEN 14511-3:2011 for chillers without the chilled water circulation pump. For a chilled water flow of 3 $m^3 \cdot h^{-1}$ the circulation pump power to be considered is 175 W

(Table 2), thus this is the value to be subtracted from the cooling capacity values deduced from the measured data.

The prototypes did not include the hot water circulation pump. For this reason, the corresponding pumping power due to pressure losses in the hot water circuit (125 W according to Table 2) was added to the electrical power input of the whole prototype. The water-cooled prototype did not include the cooling water pump either, therefore the electrical pumping power for the cooling water pump, calculated according to the prEN 14511-3:2011 standard, was added to the electrical power input of the whole prototype. These corrections are a very relevant issue for the electrical coefficient of performance (COP_{elec}) when comparing absorption chillers with conventional cooling technologies. The power consumption parameters of the external water circuits are summarized in Table 2.

Results and discussion

At the nominal operating conditions selected in this work, namely chilled water outlet temperature of 15 ºC, cooling water inlet temperature of 37.5 ºC and hot water inlet temperature of 90 ºC, the cooling capacity calculated from measured data was 10.16 ± 0.5 kW and 10.06 ± 0.5 kW for the laboratory prototype and the pre-industrial prototypes, respectively. These values of cooling capacity are before applying the corrections commented in the last paragraph according to prEN-14511:2011. Regarding the generation power, the values calculated from measured data were 15.27 ± 0.5 kW and 16.42 ± 0.5 kW for the laboratory prototype and the pre-industrial prototypes, respectively. The slightly higher value of the generation power in the pre-industrial prototype can be hardly explained because there was not a solution mass flow meter mounted within this machine. Therefore, the thermal coefficient of performance (COP_{ther}) was 0.67 ± 0.03 and 0.61 ± 0.03 for the laboratory prototype and the pre-industrial prototypes, respectively. These values of the nominal COP_{ther} obtained for the different prototypes developed in this work are significantly higher than those reported by Heard et al. (1996) and commented in paragraph 2.

Figure 3 shows the experimental data of the cooling capacity and the generation power of the air-cooled prototype depending on the ambient air temperature for two different temperatures of hot water entering the generator, namely 85ºC and 90ºC. Plotted data corresponds to the outlet temperature of chilled water of 15 ºC and nominal fan speed of 600 rpm. The thermal coefficient of performance (COP_{ther}) is 0.6 ±0.03 at ambient air temperature of 35ºC and a temperature of hot water entering the generator of 90ºC.

Figure 4 shows that, when operating at 41 ºC of ambient air temperature, the chiller is still able to provide 64 % of its nominal capacity at 35 ºC without risk of crystallization

of the solution. This confirms the major advantage of using ammonia/lithium nitrate as a working pair in air-cooled absorption chillers.

Figure 4 illustrates how, when producing chilled water at 15 ºC, for instance for cooling floor applications, there is no significant improvement of the thermal coefficient of performance (COP_{ther}) when the temperature of hot water entering the generator is increased from 85º to 100ºC. On the other hand, when producing chilled water at 8ºC, for cooling applications with fancoils, a high generation temperature is desirable, especially for high values of ambient air temperature.

To assess the effect of the refrigerant heat exchanger (RHX) on the cooling capacity, the air-cooled prototype was modified dismounting the RHX. Figure 5 shows that after dismounting the RHX an improvement of 3 % in the cooling capacity was achieved, however the difference is lower than the uncertainty measurement and no conclusion can be drawn. In any case the reduction of the number of Brazed Plate Heat Exchangers (BPHE) from 6 to 5 has a significant effect on the prototype cost.

Afterwards, the testing of the water-cooled prototype was carried out. In order to reduce the electrical consumption and therefore increase the electrical coefficient of performance (COP_{elect}) of this prototype, the original multicellular solution pump with a very low performance was replaced by a new rotary vane pump (Fluid-o-Tech PO411E) with a power consumption of 3.7 times less. The electrical coefficient of performance (COP_{elec}) of the prototype achieved with both the original and the new solution pumps is shown in Figure 6 at two temperatures of hot water entering the generator, namely 90º and 95 ºC. Higher values of the COP_{elec} with the new solution pump can be appreciated in this figure.

Finally, different water flows were set in the three external water circuits. Determining the optimal water flows is essential for operating the prototype with low power consumption and hence to achieve high COP_{elec}. As can be observed in Figure 7(a), reducing the chilled water flow ($\dot{V}_E$) from 3.0 $m^3 \cdot h^{-1}$ to 1.5 $m^3 \cdot h^{-1}$ led to an improvement of 17.7% in the COP_{elec}. Figure 7(b) shows that decreasing the hot water flow ($\dot{V}_G$) from 3.0 $m^3 \cdot h^{-1}$ to 2.0 $m^3 \cdot h^{-1}$ led to an improvement of 7.7% in the COP_{elec}. Further reduction was not worth carrying out due to the fact that the generation of ammonia is reduced and cooling capacity decreases more than pump consumption does. On the other hand, decreasing the cooling water flow ($\dot{V}_{AC}$) has a negative effect on the thermal coefficient of operation (COP_{ther}) of the prototype. Regarding the electrical coefficient of performance (COP_{elec}) there is an optimum cooling water flow at $\dot{V}_{AC}$ = 5.0 $m^3 \cdot h^{-1}$ for our operating conditions (Figure 7(c)), but the difference with the nominal value set at $\dot{V}_{AC}$ = 6.0 $m^3 \cdot h^{-1}$ was less than the uncertainty measurement; therefore the nominal flow was maintained. The significant decrease obtained in the COP_{ther} when reducing the cooling water flow rate is due to the parallel flow configuration used for cooling water in the absorber and the condenser without regulating the water flow rate passing through each heat exchanger. Provided that the size and number of plates in the condenser were smaller, the cooling water flow was not equally split between the condenser and the absorber, the flow passing through the absorber being much higher. The cooling water flow rate decrease resulted in a significant increase in the condensation pressure and a reduction of the cooling capacity. A sudden jump of 0.5 bar in the condensation pressure was measured when reducing $\dot{V}_{AC}$ from 5.0 to 4.0 $m^3 \cdot h^{-1}$. Table 3 summarizes the electrical consumption in both water-cooled and air-cooled prototypes.

After carrying out the improvement process consisting in dismounting the refrigerant heat exchanger (RHX), substituting the original multicellular centrifugal solution pump with a new one with 3.7 times less electrical consumption, and optimizing the water flows in the chilled water and hot water circuits, the performance parameters of the water-cooled prototype were: Q_E = 12.9 kW and COP_{elec} = 19.3 at 15º, 35º and 90 ºC of chilled water, cooling water and hot water temperatures, respectively. For the sake of comparison, a CIAT AGEO 40HT water-to-water vapour compression chiller with the same cooling capacity, equipped with a scroll compressor and charged with R-410A as refrigerant, has an electrical coefficient of performance ($COP_{elec)}$ of 4.6 (prEN 14511-3:2011) when producing chilled water at 15 ºC and condensing with cooling water at 35 ºC.

The corresponding performance parameters for the air-cooled prototype were: Q_E = 9.3 kW and COP_{elec} = 6.5 at 15º, 35º and 90 ºC of chilled water, ambient air and hot water temperatures, respectively, and a fan speed of 600 rpm. In order to perform a comparison with a vapour compression unit, it is worth mentioning that a CIAT AQUALIS 33H Inverter air-to-water chiller with a similar cooling capacity yields a value of 3.6 for the COP_{elec}, expressed taking the circulation pump consumption as suggested in the prEN 14511-3:2011.

Figures 8(a) and 8(b) summarize the distribution of the overall electrical consumption in the different components of both water-cooled and air-cooled prototypes.

It can be observed in Figure 8(a) that, for the water-cooled prototype, there is still room for a COP_{elec} improvement, if a better water distribution was carried out between the condenser and the absorber and a lower cooling water flow was employed.

Regarding the air-cooled prototype, Figure 8(b) shows how fan and cooling water circulation pump still represent 64% of the total electrical consumption. Different alternatives can be considered for future research for improving the COP_{elec}. Direct ammonia condensation in the finned-tube coil would save the BPHE condenser and the corresponding consumption of the cooling water circuit (Bourouis et al. 2009). Air flow could indeed be lower thanks to the higher temperature gradient (LMTD) in the coil. The drawback is that the ammonia refrigerant charge would be higher. The elimination of the cooling water circulation pump would require absorbing the ammonia in the ammonia/lithium nitrate solution directly in the coil tubes. This topic is currently being investigated by other researchers, as reported previously in paragraph 1.

Conclusions

A new ammonia/lithium nitrate absorption chiller has been developed and experimentally characterized. Two pre-industrial prototypes, a water-cooled one and an air-cooled one were built-up based on a single-effect configuration of the absorption refrigeration cycle and using brazed plate heat exchangers in all thermal components. The nominal cooling capacity of the water-cooled prototype was 12.9 kW at 15º, 35º and 90 ºC of chilled water, cooling water and hot water temperatures, respectively. The nominal cooling capacity of the air-cooled prototype was 9.3 kW at 15º, 35º and 90 ºC of chilled water, ambient air and hot water temperatures, respectively. At an ambient air temperature of 41 ºC the chiller is still able to provide 64 % of its nominal capacity at 35 ºC.

After carrying out the improvement process consisting in dismounting the refrigerant heat exchanger (RHX), substituting the original multicellular centrifugal solution pump

with a new one with 3.7 times less electrical consumption, and optimizing the water flows in the chilled water and hot water circuits, the electrical coefficient of performance (COP_{elec}) achieved with the water-cooled and air-cooled prototypes was 19.3 and 6.5, respectively.

Acknowledgements

This work has been co-funded by the *Agencia de Innovación y Desarrollo de Andalucía*, ref: IDEA-351036, and the *Corporación Tecnológica de Andalucía, ref: CTA-11/426* as a part of the CONFISOL Project.

References

[1] Amaris C., Vallès M., Bourouis M. ,Coronas A. Experimental analysis on heat and mass transfer processes in a tubular bubble absorber with ammonia/lithium nitrate for absorption chillers. Proceedings of the 21ST National & 10TH ISHMT-ASME Heat and Mass Transfer Conference, IIT Madras, India, December 27-30, 2011.

[2] Bourouis M., Coronas A., Vallès M., Zamora M. Air/water or water/water absorption water cooler using ammonia and lithium nitrate. OEPM Madrid P200930758. 29/09/2009, PCT/ES2010/070608.

[3] Cerezo J. Study of the absorption process with ammonia/water mixture in plate heat exchangers for absorption refrigeration systems (in Spanish), PhD Thesis, Rovira i Virgili University, Tarragona, Spain, 2006.

[4] Deng J., Wang R.Z., Han G.Y. (2011). A review of thermally activated cooling technologies for combined cooling, heating and power systems. Progress in Energy and Combustion Science, 37(2):172-203.

[5] Electrolux, (1930). *Improvements in or relating to Absorption Refrigerating apparatus.* Patent GB358844 (A).

[6] González-Gil A., Izquierdo M., Marcos J.D., Palacios E. (2011). Experimental evaluation of a direct air-cooled lithium bromide-water absorption prototype for solar air conditioning. Applied Thermal Engineering, 31(16):3358-3368.

[7] Heard C. L., Ayala R., Best R. An experimental comparison of an absorption refrigerator using ammonia/water and ammonia/lithium nitrate. Proceedings of International Sorption Heat Pump Conference, Montreal, Canada, September 17-20, 1996.

[8] Infante Ferreira C.A. (1984). Thermodynamic and physical property data equations for ammonia-lithium nitrate and ammonia-sodium thiocyanate. Solar Energy, 32(2):231-236.

[9] Jakob U., Kohlenbach P. Recent developments of sorption chillers in Europe. Proceedings of the 9th IIR Gustav Lorentzen Conference, Sydney, Australia, April 12-14, 2010.

[10] Kim D.S., Infante Ferreira C.A. (2009). Air-cooled LiBr–water absorption chillers for solar air conditioning in extremely hot weathers. Energy Conversion and Management, 50(4):1018–1025.

[11] Kim D.S., Machielsen C.H.M. Evaluation of air-cooled solar absorption cooling systems. Proceedings of the International Sorption Heat Pump Conference, Shanghai, China, September 24-27, 2002.

[12] KLEIN, S.A. (2007). Engineering Equation Solver (1992-2007). V8.017-3D

[13] Libotean S., Salavera D., Vallès M., Esteve X., Coronas A. (2007). Vapour-Liquid Equilibrium of Ammonia+Lithium Nitrate+Water and Ammonia+Lithium Nitrate Solutions from (293.15 to 353.15) K; J. Chem. Eng. Data, 52:1050-1055.

[14] Libotean S., Martín A., Salavera D., Vallès M., Esteve X., Coronas A. (2008). Densities, Viscosities, and Heat Capacities of Ammonia + Lithium Nitrate and Ammonia + Lithium Nitrate + Water Solutions between (293.15 and 353.15) K. J. Chem. Eng. Data, 53(10):2383–2388.

[15] Llamas U., Best R., Bujedo L.A., Melograno P., Velázquez N., Piltatowski I. First Experimental Results of a Solar Driven Ammonia-Lithium Nitrate Cooling System. Proceedings of the 4th International Conference Solar Air-Conditioning, Larnaka, Cyprus, ISBN 978-3-941785-48-9, October 12-14, 2011.

[16] Marcos J.D. Air-cooled LiBr/H_2O double-effect absorption cooling prototype. Simulation, Optimization and experimental results (in Spanish), PhD Thesis, University Carlos III of Madrid, Spain, 2008.

[17] Oronel C. Experimental study of the absorption and desorption processes of $NH_3/LiNO_3$ and $NH_3/(LiNO_3+H_2O)$ in plate heat exchangers for absorption refrigeration systems (in Spanish), PhD Thesis, Rovira i Virgili University, Tarragona, Spain, 2010.

[18] Sun D.W. (1998). Comparison of the performances of NH_3-H_2O, NH_3-$LiNO_3$, and NH_3-NaSCN absorption refrigeration systems. Energy Conversion and Management, 39(5-6):357-368.

[19] Táboas F. Study of the flow boiling process of ammonia/water mixture in plate heat exchangers for absorption refrigeration systems (in Spanish), PhD Thesis, Rovira i Virgili University, Tarragona, Spain, 2006.

[20] Venegas M., Rodríguez P., Lecuona A., Izquierdo M. (2005). Spray absorbers in absorption systems using lithium nitrate-ammonia solution. International Journal of Refrigeration, 28(4):554-564.

[21] Ventas R., Lecuona A. (2010). Legrand M., Rodriguez-Hidalgo M.C. On the recirculation of ammonia-lithium nitrate in adiabatic absorber for chillers. Applied Thermal Engineering, 30(17-18):2770-2777.

[22] Zacarías A., Ventas R., Venegas M, Leucona A. (2010). Boiling heat transfer and pressure drop of ammonia-lithium nitrate solution in a plate generator. International Journal of Heat and Mass Transfer, 53:4768-4779.

[23] Zacarías A., Venegas M., Ventas R., Leucona A. (2011). Experimental assessment of ammonia adiabatic absorption into ammonia-lithium nitrate solution using a flat fan nozzle. Applied Thermal Engineering, 31(16):3569-3579.

[24] Zamora M., Bourouis M., Vallès M., Coronas A. A new ammonia/lithium nitrate absorption chiller for solar cooling applications. Proceedings of the International Conference on Ammonia Refrigeration Technology, Ohrid, Macedonia, ISBN 978-2-913149-85-4, April 14-16, 2011.

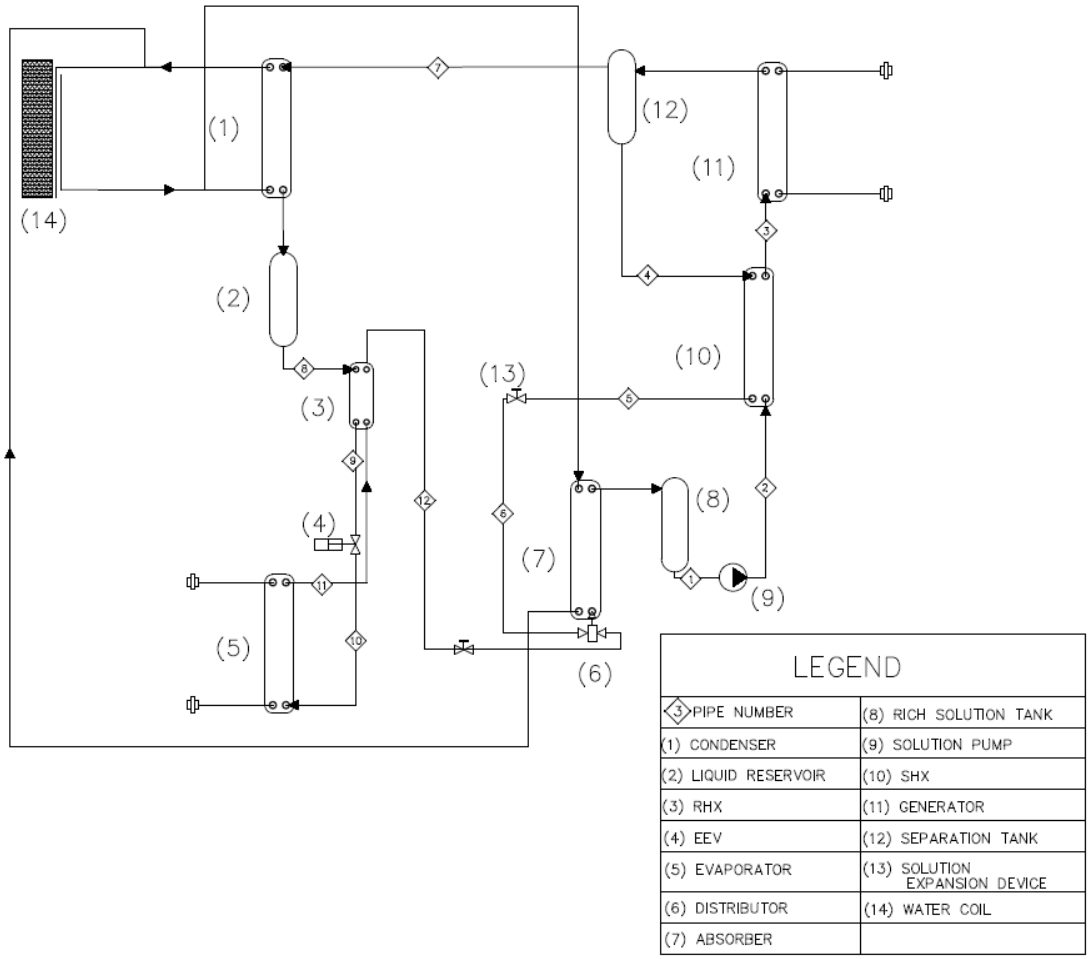

Figure 1. Configuration of the absorption refrigeration cycle employed for the developed prototypes (Adapted from Bourouis et al. 2009)

Figure 2. Air-cooled prototype in the climatic chamber testing facility

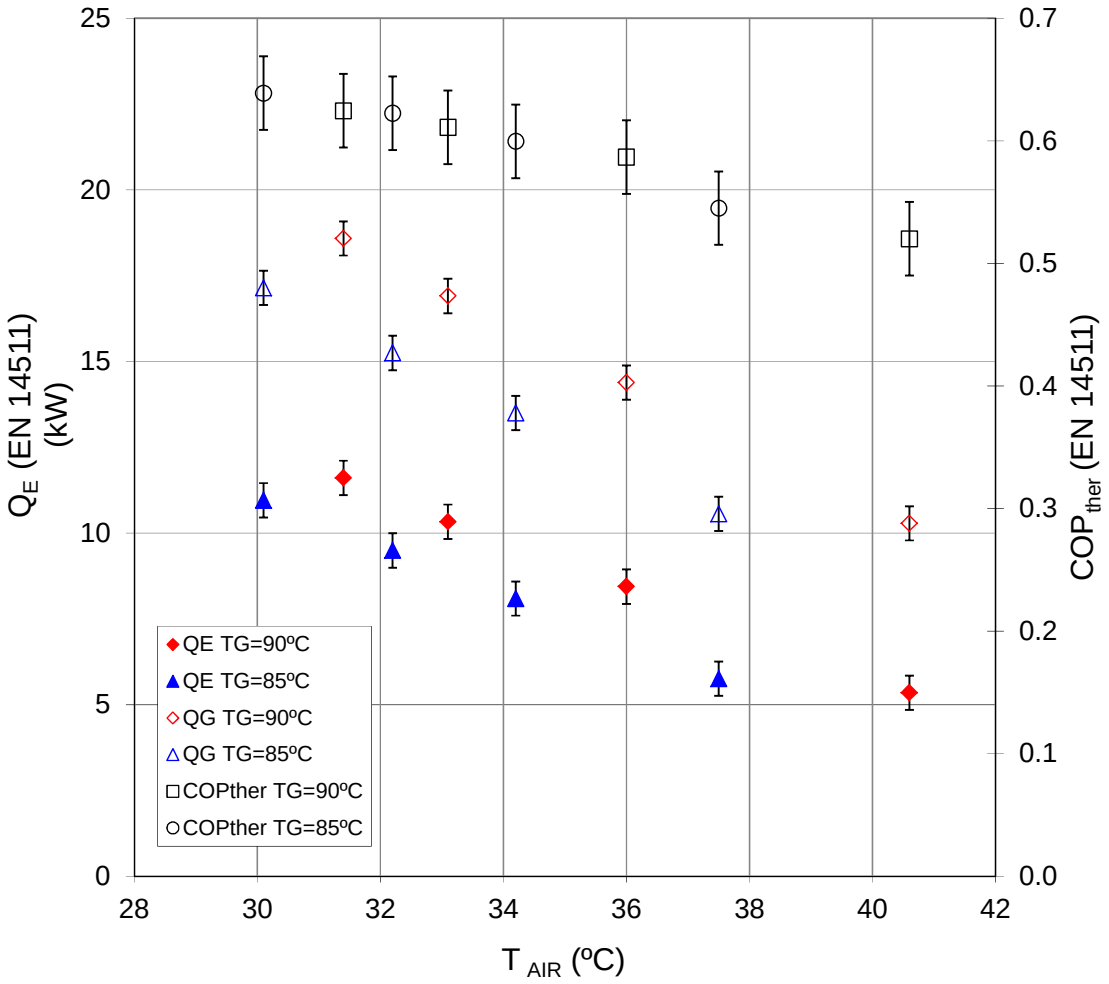

Figure 3. Cooling capacity, generation power and thermal coefficient of performance versus ambient air temperature for the air-cooled prototype

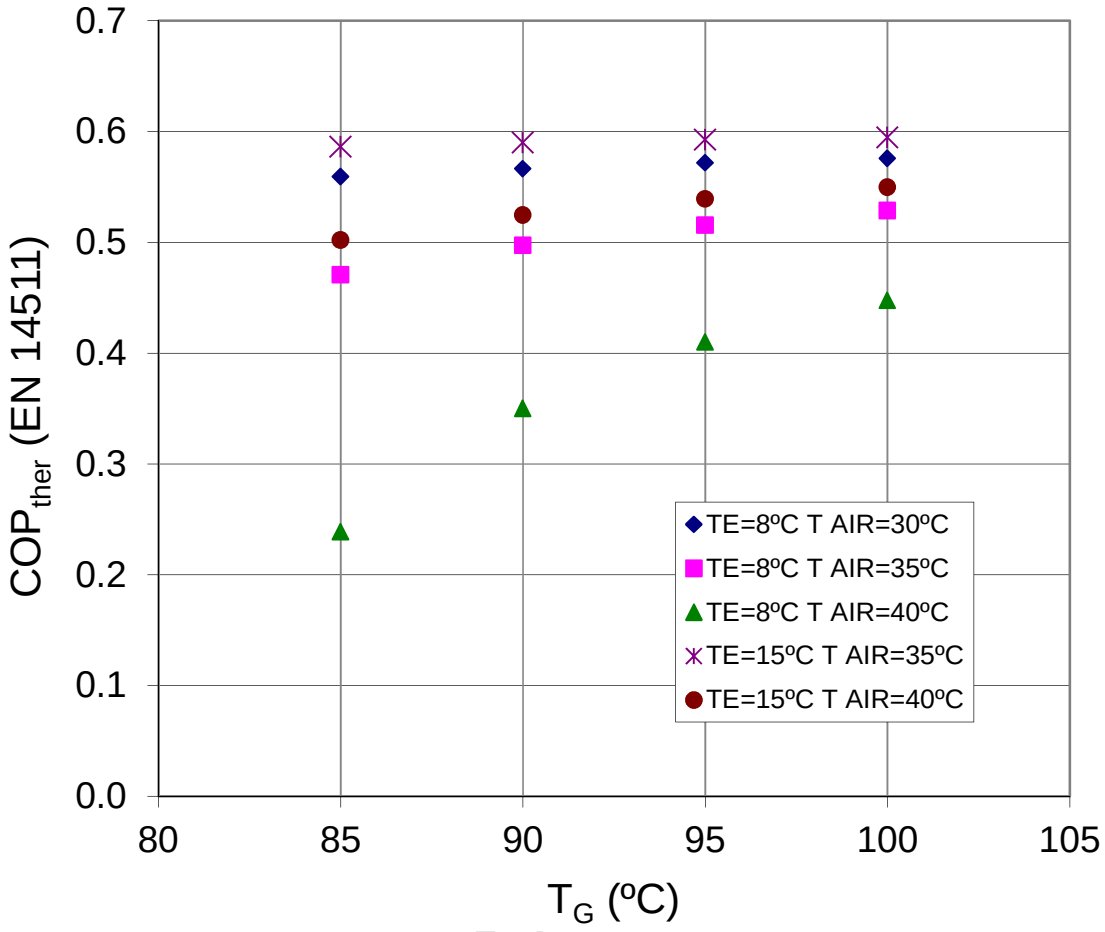

Figure 4. Thermal coefficient of performance versus hot water temperature at chilled water temperatures of 8º and 15 ºC, ambient air temperatures of 30º, 35º and 40 ºC and a fan speed of 600 rpm

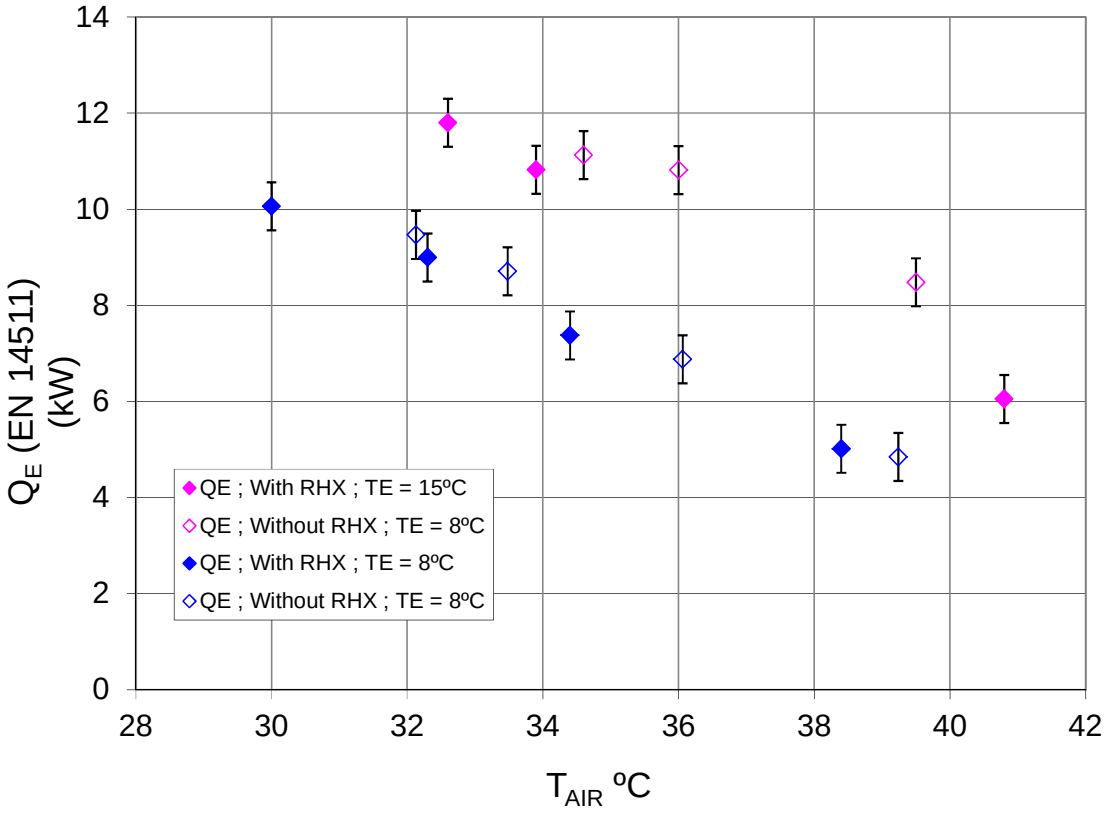

Figure 5. Cooling capacity of the air-cooled prototype, with and without RHX, versus the ambient air temperature at chilled water temperatures of 8º and 15 ºC, hot water temperature of 90 ºC and a fan speed of 600 rpm

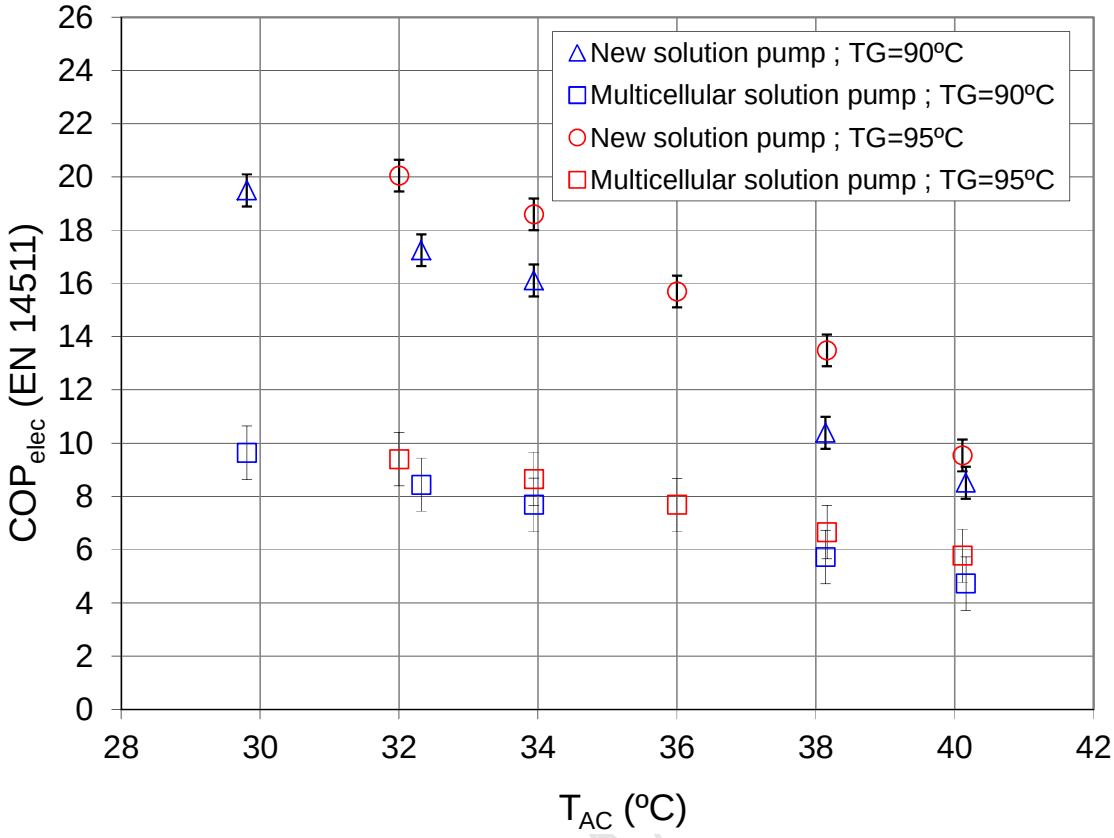

Figure 6. Electrical coefficient of performance versus the cooling water temperature for both solution pumps tested at hot water temperatures of 90º and 95 ºC and a chilled water temperature of 5.4 ºC

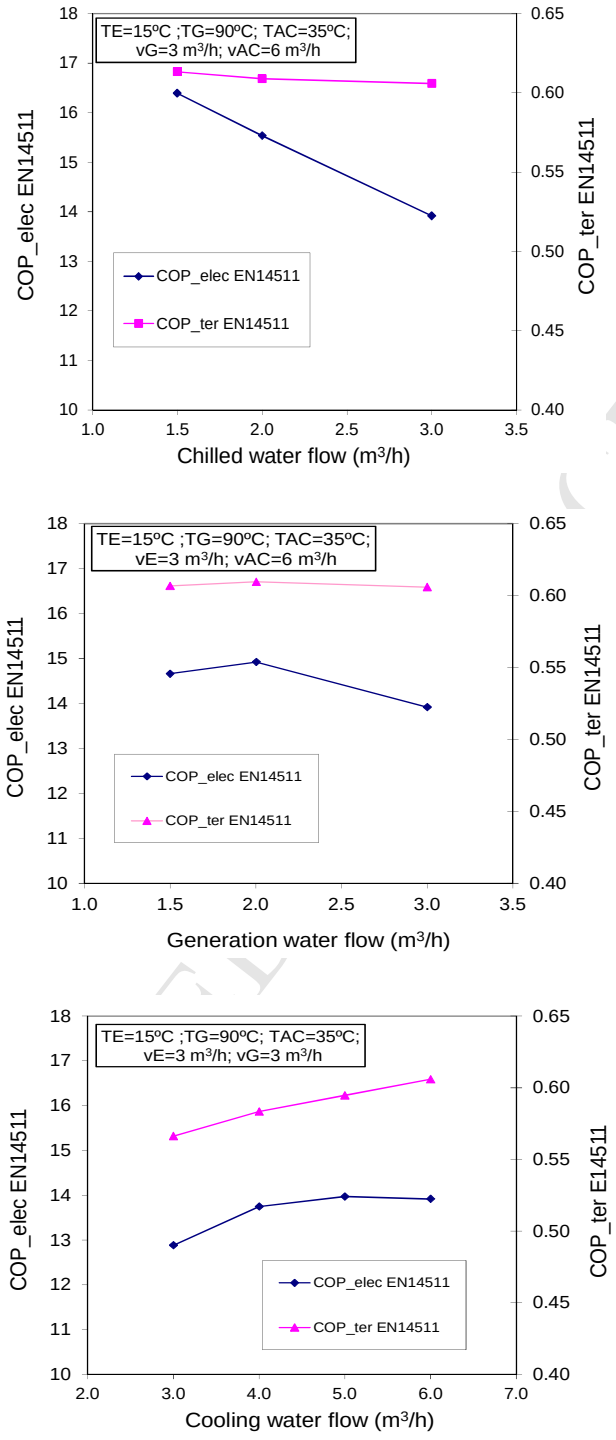

Figure 7. Thermal and electrical coefficients of performance versus the water flows of the external circuits: (a) chilled water flow; (b) hot water flow; (c) cooling water flow

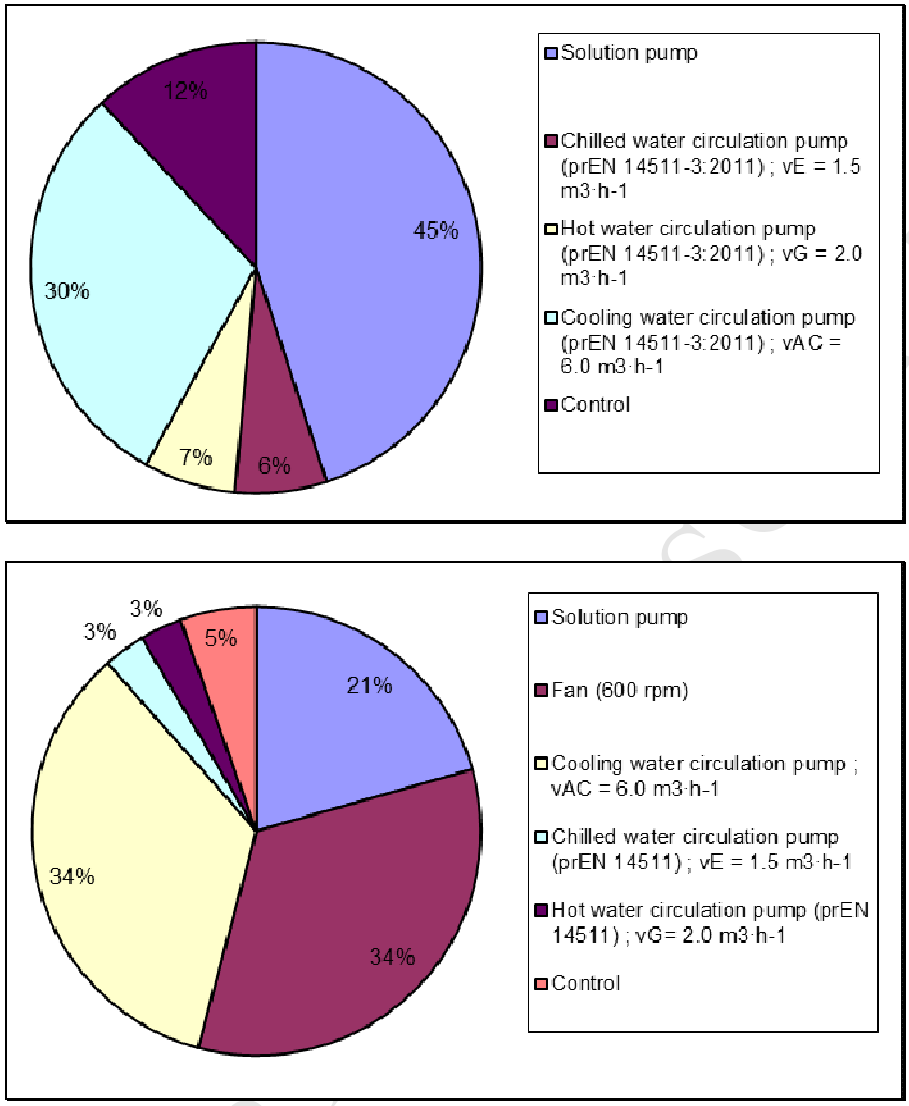

Figure 8. Distribution of the total electrical consumption in the different components of the absorption chiller: (a) water-cooled prototype; (b) air-cooled prototype

Figures caption

Figure 1. Configuration of the absorption refrigeration cycle employed for the developed prototypes (Adapted from Bourouis et al. 2009)

Figure 2. Air-cooled prototype in the climatic chamber testing facility

Figure 3. Cooling capacity, generation power and thermal coefficient of performance versus ambient air temperature for the air-cooled prototype

Figure 4. Thermal coefficient of performance versus hot water temperature at chilled water temperatures of 8º and 15 ºC, ambient air temperatures of 30º, 35º and 40 ºC and a fan speed of 600 rpm

Figure 5. Cooling capacity of the air-cooled prototype, with and without RHX, versus the ambient air temperature at chilled water temperatures of 8º and 15 ºC, hot water temperature of 90 ºC and a fan speed of 600 rpm

Figure 6. Electrical coefficient of performance versus the cooling water temperature for both solution pumps tested at hot water temperatures of 90º and 95 ºC and a chilled water temperature of 5.4 ºC

Figure 7. Thermal and electrical coefficients of performance versus the water flows of the external circuits: (a) chilled water flow; (b) hot water flow; (c) cooling water flow

Figure 8. Figure 8. Distribution of the total electrical consumption in the different components of the absorption chiller: (a) water-cooled prototype; (b) air-cooled prototype

Table 1. Operating conditions employed for testing the air-cooled prototype

Controlled variable	**Measurement Rage**
T_{E2} [ºC]	8.0 – 15.0
T_{G1} [ºC]	85.0 – 90.0 – 95.0
F [rpm]	1020 – 800 – 600 – 400
T_{AIR1} [ºC]	Range (30.0 to 42.0)
$\dot{v}_E$ [$m^3 \cdot h^{-1}$]	3.0
$\dot{v}_G$ [$m^3 \cdot h^{-1}$]	3.0
$\dot{v}_{AC}$ [$m^3 \cdot h^{-1}$]	Not measured
$\dot{v}_{AIR}$ [$m^3 \cdot h^{-1}$]	Not measured

Table 2. Power consumption of the circulation pumps in the external circuits to be taken into account in the total electrical consumption of the chiller

Pumping Power; EN 14511-3:2011					
	$\dot{V}$ [$m^3 \cdot h$]	ΔP_w [bar]	Pw_{hydra} [W]	η	Pw_{pump} [W]
Evaporator water circuit	3.0	0.496	41.32	0.24	175*
Generator water circuit	3.0	0.3	25	0.2	125
Cooling water circuit	6.0	0.3	50.0	0.25	200

* This value must be subtracted from the cooling capacity

Table 3: Summary of the electrical consumption [kW] for both water-cooled and air-cooled prototypes

Water-Cooled Prototype	
Solution pump	0.3
Chilled water circulation pump (prEN 14511-3:2011) ; $\dot{V}_E = 1.5\ m^3 \cdot h^{-1}$	0.044
Generation water circulation pump (prEN 14511-3:2011) ; $\dot{V}_G = 2.0\ m^3 \cdot h^{-1}$	0.044
Cooling water circulation pump (prEN 14511-3:2011) ; $\dot{V}_{AC} = 6.0\ m^3 \cdot h^{-1}$	0.2
Control	0.08
Total electrical consumption (kW)	0.668
Air-Cooled Prototype	
Solution pump	0.3
Fan (600 rpm)	0.49
Cooling water circulation pump ; $\dot{V}_{AC} = 6.0\ m^3 \cdot h^{-1}$	0.5
Chilled water circulation pump (prEN 14511) ; $\dot{V}_E = 1.5\ m^3 \cdot h^{-1}$	0.044
Generation water circulation pump (prEN 14511) ; $\dot{V}_G = 2.0\ m^3 \cdot h^{-1}$	0.044
Control	0.08
Total electrical consumption (kW)	1.458